Protein Engineering vol.10 no.12 pp.1425–1432, 1997

Structural and functional roles of a conserved proline residue in the α2 helix of *Escherichia coli* thioredoxin

Frédéric de Lamotte-Guéry[1,2], Christian Pruvost[3], Philippe Minard[4], Marc-André Delsuc[3], Myroslawa Miginiac-Maslow[1], Jean-Marie Schmitter[5], Mariana Stein[1] and Paulette Decottignies[1,6]

[1]Institut de Biotechnologie des Plantes, ERS 569 CNRS, Université Paris XI, 91405 Orsay, [3]Centre de Biochimie Structurale, Faculté Pharmacie, 34060 Montpellier, [4]Laboratoire d'Enzymologie Physicochimique Moléculaire, Université Paris XI, 91405 Orsay and [5]Laboratoire de Biochimie, Ecole Polytechnique, 91128 Palaiseau, France
[2]Present address: Unité de Biochimie et Biologie Moléculaire des Céréales, INRA, 34060 Montpellier, France

[6]To whom correspondence should be addressed

Proline 40 in *Escherichia coli* thioredoxin is located close to the redox active site (Cys32–Cys35) within the α2 helix. The conservation of this residue among most of the thioredoxins suggests that it could play an important role in the structure and/or function of this protein. We have substituted Pro40 for Ala by using site-directed mutagenesis and expressed the mutant P40A in *E.coli*. The effects of the mutation on the biophysical and biological properties of thioredoxin have been analyzed and compared with molecular dynamics simulations. Modeling predicted that the replacement of Pro40 by Ala induced a displacement of the active site which exposes Trp31 to the solvent and opens a cleft located between helices α2 and α3. The solvation free energy (SFE) calculation also indicated that P40A became more hydrophobic as W31 became more accessible. These predictions were totally in agreement with the experimental results. The mutant P40A exhibited chromatographic behavior and fluorescence properties very different from those of the wild-type (WT) protein, in relationship with the displacement of W31. The determination of the free energy of unfolding of P40A showed that the mutant was globally destabilized by 2.9 kcal/mol. However, the effect of the mutation on the transition curve was highly unusual as the midpoint of the unfolding transition increased, indicating that some local structures were actually stabilized by the mutation. Despite these structural modifications, neither the ability of the protein to reduce a chloroplastic enzyme nor its reactivity with the bacterial reductase decreased. The only functional difference was the higher stability of P40A in light activation of NADP–malate dehydrogenase under air, which suggests that the mutant was less rapidly re-oxidized than WT. Therefore, it can be concluded that Pro40 is not essential for maintaining the redox function of thioredoxin but rather is required for the stability of the protein.

Keywords: α-helix/NADP–malate dehydrogenase activation/protein stability/site-directed mutagenesis/thioredoxin

Introduction

Thioredoxins are small molecular mass (12 kDa) heat-stable proteins containing a readily reducible disulfide bridge with the amino acid sequence Cys–Gly–Pro–Cys. Through their isolation and characterization from numerous species, thioredoxins have been found to play a role in physiological processes as diverse as blood clotting, division and proliferation of animal cells, germination of seeds and regulation of photosynthesis (for a review, see Buchanan *et al.*, 1994).

At the molecular level, thioredoxins serve as hydrogen donors in a wide variety of reactions, such as ribonucleotide reduction (Laurent *et al.*, 1964) and methionine sulfoxide reduction (Gonzalez Porque *et al.*, 1970). They also modulate the activity of transcription factors NF-kB and AP-1 (Schenk *et al.*, 1994). Their function as general protein disulfide reductases has been well demonstrated in the cases of insulin (Holmgren, 1979) and several chloroplast enzymes including NADP–malate dehydrogenase (NADP–MDH), phosphoribulokinase and fructose-1,6-bisphosphatase (Buchanan, 1991). In addition to their redox function, thioredoxins have been shown to play a structural role in several systems. *Escherichia coli* thioredoxin is required for the replication of T7 bacteriophage, as a subunit of the T7 DNA polymerase complex (Tabor *et al.*, 1987) and is essential for the assembly of the filamentous phages M13 and f1 (Russel and Model, 1985). In these two cases, mutagenesis experiments have shown that the disulfide bridge of thioredoxin is not required (Russel and Model, 1986), whereas it is essential for chloroplast enzyme activation (Jacquot and Decottignies, 1986). The three-dimensional structure of oxidized *E.coli* thioredoxin has been solved by X-ray crystallography (Holmgren *et al.*, 1975; Katti *et al.*, 1990) and the structure of the reduced protein elucidated by NMR (Dyson *et al.*, 1989). Reduced and oxidized thioredoxins have identical secondary structures and tertiary folds, consisting of a central five-stranded β-sheet with two parallel junctions and two antiparallel junctions. This central sheet is surrounded by α-helices. The active site disulfide (Cys32–Cys35) is located in a short loop at the amino end of the α2 helix, after the second strand of the β-sheet.

Most of the highly conserved residues have been extensively studied. The role of the active cysteines and also the amino acids surrounding the active site, Pro34, Lys36 and Trp31, has been investigated (Kelley and Richards, 1987; Gleason *et al.*, 1990; Krause and Holmgren, 1991). Asp 26, buried in the core of the protein, has been scrutinized by several groups (Langsetmo *et al.*, 1991; Ladbury *et al.*, 1993). Among the conserved residues, Pro40 is present in all thioredoxins sequenced so far, except a chloroplast-encoded thioredoxin present in a red alga (Reynolds *et al.*, 1994) and the two h-type thioredoxins from *Nicotiana tabacum* (Brugidou *et al.*, 1993). This residue is located in the α2 helix and it has been proposed that it maintains the conformation of the active disulfide (Eklund *et al.*, 1991). It is well known that the proline ring cannot easily maintain the H-bonding pattern of the α-helix backbone and is a very effective helix stop (Strehlow *et al.*, 1991). In *E.coli* thioredoxin, the presence of Pro40 does not stop the helical structure but induces a kink which separates

the active site cysteine residues of the α2 helix from the rest of the structure. The consequence is that the active disulfide is exposed at the surface of the protein.

In the present study, we have substituted Pro40 for an alanine by site-directed mutagenesis in order to investigate the role of this residue, both functionally and structurally. The P40A mutant has been compared with the wild-type protein using a wide range of enzymatic and physicochemical tests. These results have been interpreted in the light of a molecular dynamics simulation.

Materials and methods

Modeled structures of P40A and WT thioredoxins

The X-ray structure of thioredoxin (Katti *et al.*, 1990) was the starting point of all the simulations, which were performed on the reduced form of native and mutant proteins. The P40A substitution was built by mutating directly proline 40 into an alanine. Both structures were minimized before further use. The solvent was incorporated as a 25 Å sphere around the solute centre of mass, comprising 1540 water molecules. The hydrogen charge in water was set to 0.417 C. The solute–solvent ensemble was equilibrated by alternating steps of energy minimization and 10 K dynamics. The minimization was first applied to the water molecules, then extended progressively to the solute hydrogens, side chains and finally the protein backbone. A 400 ps dynamics in water was performed at 300 K with a 200 fs contact time and a 1 fs step. The simulation was started at 10 K and the system was allowed to reach the bath temperature in 20 ps. A distance-dependent dielectric function, $e = r_{ij}$ and a cut-off distance of 10 Å for the non-bonded interactions were used. The results were analyzed for the last 100 ps after stabilization of the total energy and root mean square deviation (r.m.s.d.) from the starting structure.

The simulations were performed using the program Amber 4.0. The programs InsightII and Access (Eisenberg and McLachan, 1986) were used for comparison and first evaluation of the structures and for the solvation free energy (SFE) estimation, the solvent accessibility surface calculations. The helix angle was approximated by the angle between two lines, each of them positioned in the direction of the helix axis on each side of the helix. All the calculations were performed on a Hewlett-Packard HP735 computer under OS HPUX 9.01.

Enzymes. NADPH thioredoxin reductase and thioredoxin from *E.coli* were purchased from IMCO (Stockholm, Sweden). NADP–MDH, ferredoxin and ferredoxin–thioredoxin reductase were purified as described (Decottignies *et al.*, 1988).

Bacterial strain and vectors. TG2 (supE hsdΔ5 thi Δ(lac-proAB) Δ(srl-recA)306 :: Tn10 (tet^r); F′ [traD36 pro AB^+ $lacI^q$ lacZΔm15] was used for M13 (Pharmacia) and BlueScript KS II plasmid (Stratagene) preparation, and also for thioredoxin overexpression. Bacteria were grown in Luria–Bertani medium with ampicillin at a final concentration of 50 μg/ml when necessary.

Construction of mutations. The *KpnI*/*PstI* fragment containing the *trxA* gene from *E.coli* strain K38 and its regulatory sequences was inserted into M13 mp19. Single-stranded DNA was used as a template for site-directed mutagenesis (Kunkel, 1985). A 21-base deoxyoligonucleotide was synthesized complementary to the coding strand with the following sequence (mismatch underlined): ATC CAG AAT G<u>C</u><u>G</u> GGG GAT CAT. The replicative form DNA of one positive clone was used to transfer the *trxA* gene into pFP1 (de Lamotte-Guéry *et al.*, 1991).

Production and purification of wild-type and mutant thioredoxins. Mutant and wild-type thioredoxins were expressed and purified as described previously (de Lamotte-Guéry *et al.*, 1991) using the pFP1 overexpression plasmid. Thioredoxin P40A was further purified on a TSK phenyl 5PW column (0.75 cm×7.5 cm) (LKB) by using a 40 min linear decreasing gradient of ammonium sulfate (0.9–0 M) in 0.1 M sodium phosphate, pH 7.2. The flow rate was 1 ml/min. Thioredoxin concentrations were determined from the absorbance at 280 nm, using 12 650 l/mol.cm as the molar absorption coefficient. The purity of the preparations was determined by SDS–PAGE and native gels. Commercial wild-type thioredoxin was used as a standard.

Control of the mutation. (1) Tryptic mapping and sequencing. Thioredoxins WT and P40A (8 nmol) were reduced with 3.5 mM dithiothreitol (DTT) for 30 min at 37°C and carboxymethylated with 5 mM [1-^{14}C]iodoacetic acid for 15 min in the dark. The reaction was stopped with 30 mM 2-mercaptoethanol and the reagents in excess were removed using a Centricon 10 microconcentrator (Amicon). In the same process the phosphate buffer was replaced by 0.1 M NH_4HCO_3, pH 8.3. ^{14}C-carboxymethylated thioredoxins were cleaved with trypsin (1:40, w/w) for 5 h at 37°C. The digest was purified by reversed-phase liquid chromatography on a C_4 column (0.46 cm×15 cm) (Vydac) with a 90 min linear gradient over 0–70% CH_3CN in 0.1% trifluoroacetic acid. The peptide containing the mutated amino acid was sequenced using an Applied Biosystems Model 470 A sequencer.

(2) Electrospray mass spectrometry. Thioredoxins, previously desalted by reversed-phase liquid chromatography, were analyzed with a VG BioQ mass spectrometer, using a 20 pmol/ml protein solution in formic acid–methanol–water (1:5:5).

Reversed-phase liquid chromatography. Thioredoxins were chromatographed on a C_4 column (0.46 cm×15 cm) (Vydac). Elution was performed with a 30 min linear gradient from 42 to 56% CH_3CN in 0.1% trifluoroacetic acid, at a flow rate of 1 ml/min.

Fluorescence measurements. Spectra were recorded using a Perkin-Elmer MPF-44B fluorimeter at 20°C in a 1 cm pathlength cell in a total volume of 1 ml containing 10 mM phosphate buffer, pH 7.2, and 7 μM thioredoxin. The excitation wavelength was 280 nm and emission was recorded from 280 to 400 nm. Reduction was performed with 5 mM DTT for 10 min at 20°C.

Circular dichroism. Spectra were recorded from 185 to 250 nm using a Jobin-Yvon Mark IV dichrograph at 20°C. Measurements were made in a 0.2 cm pathlength cell in a total volume of 0.7 ml of 10 mM phosphate buffer, pH 7.2, containing 7 μM thioredoxin. Reduction was performed with 5 mM DTT for 10 min at 20°C. Data were analyzed using the method of Chang *et al.* (1978).

Denaturation and renaturation experiments. Thioredoxin samples (5 μM) in 25 mM phosphate buffer, pH 7.2, were equilibrated overnight at 25°C in the presence of variable concentrations of Gdn–HCl (0–6 M). Fluorescence and circular dichroism spectra were recorded as described above. For renaturation experiments, oxidized samples were denatured

with 6 M Gdn–HCl overnight, then diluted with buffer at various concentrations.

Enzyme assays. (1) Reduction by thioredoxin reductase (Slaby and Holmgren, 1975). Thioredoxins were tested as substrates of *E.coli* NADPH–thioredoxin reductase in a final volume of 1 ml containing 100 mM phosphate buffer, pH 7.1, 10 mM EDTA, 150 μM NADPH, 500 μM 5,5′-dithiobis(2-nitrobenzoic acid) and variable amounts (0.3–12 μM) of thioredoxin. The reaction was started by adding 10 nM of thioredoxin reductase and was monitored by measuring the absorbance change at 412 nm. The activity was expressed as micromoles of thioredoxin reduced per minute, using 13 600 l/mol.cm as the molar absorption coefficient of DTNB.

(2) DTT-dependent activation of corn leaf NADP–MDH. The enzyme was activated in 30 μl of medium containing 100 mM Tris–HCl, pH 7.9, 10 mM DTT, 0.6 μM NADP–MDH and thioredoxin (0.6–22 μM). After incubating for 3 min at 20°C, an aliquot of 10 μl was used to determine the activity of NADP–MDH at 30°C in a reaction medium (1 ml) containing 100 mM Tris–HCl buffer, pH 7.9, 0.15 mM NADPH and 0.7 mM oxaloacetic acid. NADPH oxidation was monitored by measuring the decrease in absorbance at 340 nm.

(3) Light activation of corn leaf NADP–MDH. The enzyme was activated in 200 μl of mixture containing 100 mM Tris–HCl, pH 7.9, pea leaf thylakoids (equivalent to 85 μg of chlorophyll), 12 μM spinach ferredoxin, 2 μM ferredoxin–thioredoxin reductase, 0.5 μM NADP–MDH and variable amounts (1–20 μM) of thioredoxin, at 25°C under illumination (400 μmol quanta/m^2.s). At intervals, 30 μl aliquots were withdrawn to measure the activity of NADP–MDH as described above.

Results

Modeled structure analysis of P40A and WT thioredoxin

Comparison of minimized forms. Refined P40A and WT thioredoxin structures, minimized in spheres of water, were analyzed. The total energy during refinement reached a minimum point of –5750 kcal/mol for the WT and –5780 kcal/mol for the P40A with an average r.m.s.d. of 0.01 Å for both structures.

Analysis and comparison of trajectories, structure evolution. The molecular dynamics protocol was applied on both WT and mutant structures. Considering the overall trajectories, the global structure remained conserved between the P40A and WT proteins (data not shown). The two structures kept their overall fold, with the conservation of the global shape and the secondary structures, except for the small N-terminal β1 strand, which appeared to be slightly more flexible in the mutant protein. The other β strands were very well conserved with a backbone r.m.s.d. of 1.54 Å. All the helices remained highly structured and conserved during the simulations. The α1 helix was less conserved during the dynamics of the mutant protein (r.m.s.d. = 1.38 Å) because of a small orientation difference due to the shift of the β1 strand. A striking effect of the substitution was observed in the α2 helix, which became straighter in P40A (r.m.s.d. = 0.91 Å), shifting the active site and pulling on the entire structure. The α3 and α4 helices (named according to Katti *et al.*, 1990) did not change substantially (r.m.s.d. = 0.66 and 0.88 Å), but the C-terminal α4 helix moved a little along its axis with a very well conserved geometry.

Some differences in the α2 helix could be seen around the location of the Pro40 mutation. The hydrogen bond network was more important in the α2 helix of the mutant, allowing this helix to approach a more regular structure in the simulations. The angle in this helix was 59° in WT and 13° in P40A (Figure 1).

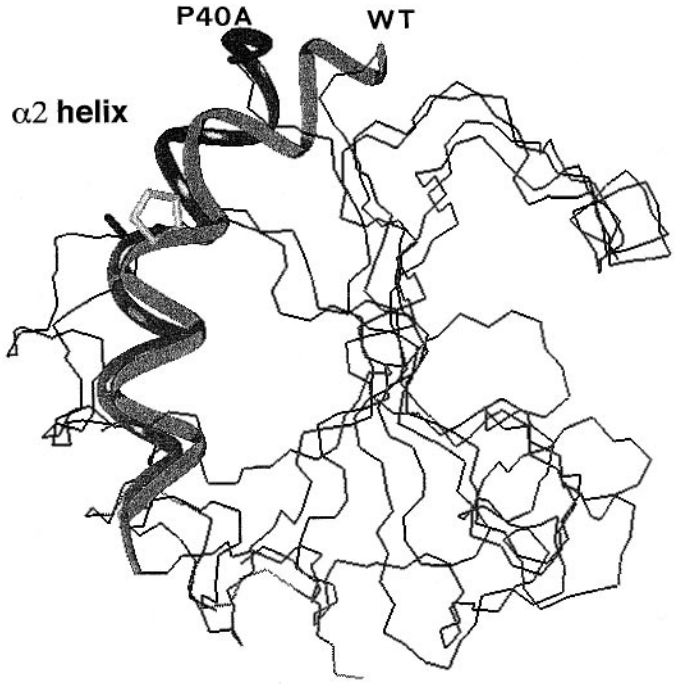

Fig. 1. Representation of the average structures and the α2 helix shape in P40A with Ala in position 40 and in WT thioredoxin with Pro in position 40 after superimposition of the β sheets (r.m.s.d. = 1.54 Å).

The mutation did not modify the structure of the active site, for which internal geometry was very well conserved ($r.m.s.d._{res31.35}$ = 0.93 Å and $r.m.s.d._{res32.35}$ = 0.27 Å on the backbone), but moved from its original position by about 6 Å (Figure 2). The shift of the active site entailed very different contacts in the two structures in the vicinity of the active site. The most striking differences concerned W31. The hydrophobic bridge binding W31 and the loop between β2 and α3 was suppressed in P40A, deleting the contacts with I5, E30, I60, Q62, N63, P64 and I72. This modification induced many changes in hydrogen bonds, for instance: in the mutant thioredoxin, W31–HNE:::I60–O and W31–HNE:::D61–OD2 disappeared, W28–HNE:::K57–O was weakened and W28–HN:::K57–O appeared (Figure 3). Those changes drastically modified the mobility of W31. This residue appeared to be very static in the WT structure, stuck to a hydrophobic patch constituted of I60, P64 and I72, whereas in P40A it was detached from the molecule surface and free to move (Figure 4). Whereas the mean distance between the two indole rings of W28 and W31 varied only from 9.64 Å (WT) to 10.54 Å (P40A), the mean angle between their planes changed drastically from 16 to 94°. We calculated the solvent access surface for the tryptophan residues during the last 100 ps (data not shown). The mean solvent access surface increased from 45.5 to 74.4 $Å^2$ for W28 and from 112.7 to 233.0 $Å^2$ for W31. The mean solvation free energy (SFE) was calculated also on the last 100 ps, showing a more hydrophilic surface for WT with a difference of 2.9 kcal/mol.

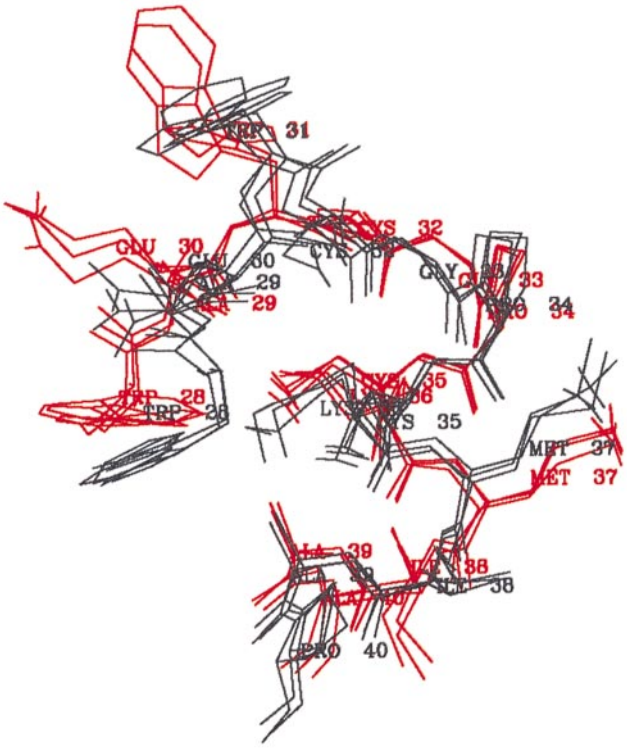

Fig. 2. Overview of the superimposition of the active site in P40A (red) and WT (black) thioredoxins.

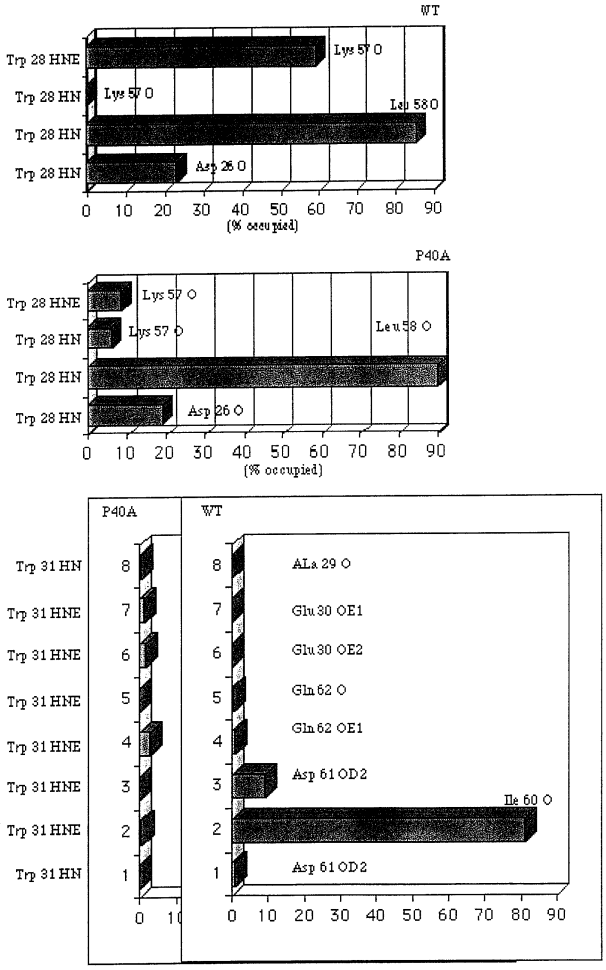

Fig. 3. H-bond presence on tryptophans Trp28 and Trp31 during the last 100 ps of dynamic simulations.

Purification of WT and P40A thioredoxins and control of the mutation

After sequencing the *trxA* gene and subcloning in pFP1, *E.coli* WT and P40A thioredoxins were purified by heat treatment, ammonium sulfate precipitation, gel filtration and anion-exchange chromatography. Such a procedure allowed us to obtain WT thioredoxin in a pure form, but P40A had to be purified further by hydrophobic interaction chromatography, because it contained a small amount of the endogenous WT protein. Thioredoxin activity was monitored during purification by using the DTT-dependent NADP–MDH activation test. After these steps, a single band was observed on SDS–PAGE and on native gels (data not shown) for both P40A and WT proteins. The mutant thioredoxin was analyzed by protein sequencing, which revealed the sequence Ser–Asp–Lys–Ile–Ile–His–Leu–Thr–Asp–Asp..., which is the expected N-terminal sequence for *E.coli* thioredoxin.

The replacement of a proline residue by an alanine does not change the number of sites cleaved by trypsin. Thus, the patterns of the tryptic mixtures were expected to be identical or almost identical for WT and P40A. Only one peptide had a slightly different retention time when the two RP-HPLC profiles were compared (data not shown). This peptide had been shown previously by mass spectrometry to correspond to the stretch M37 to K52. When sequenced, the fragment derived from P40A revealed the expected mutation, i.e. ^{37}MIAAILDE...

P40A and WT were also analyzed by electrospray mass spectrometry. The measured mass of WT was 11 674.8 ± 0.7 Da (data not shown), compared with the calculated mass of 11 675.4 Da. The measured mass of P40A (data not shown) was 11 648.9 ± 0.5 Da (calculated mass 11 649.4 Da). Therefore, the difference in mass was in good agreement with the performed mutation and we could conclude that the mutant protein contained only one modification, the replacement of Pro40 by an alanine residue. In addition, these data confirmed that the purified P40A preparation was no longer contaminated by the WT protein.

Physicochemical characterization of P40A

The CD spectra of oxidized and reduced thioredoxins were recorded and revealed no difference between the wild-type and mutated thioredoxins (data not shown). This suggests that the amino acid substitution did not alter the overall secondary structure of the protein.

The observation that P40A was easily separated from contaminating WT thioredoxin on a hydrophobic interaction column during the purification prompted us to investigate the chromatographic behavior of WT and P40A more thoroughly. A mixture of the two purified proteins could be resolved on a C_4 reversed-phase column, exhibiting very different retention times (16.7 min for WT and 22.2 min for P40A under the conditions described in Materials and methods). When reduced, both proteins eluted earlier from this column, as already observed (Wetterauer *et al.*, 1992), but were separated as efficiently as the oxidized forms.

Fluorescence emission spectra of oxidized and reduced WT and P40A thioredoxins were recorded (Figure 5). The fluorescence of oxidized WT was low, as expected since fluorescence is usually quenched in the WT under these conditions (Holmgren, 1972). A fourfold increase was observed

Fig. 4. Superimposition of 10 structures of P40A (red) and WT (black) thioredoxins during the last 100 ps of the dynamic simulations, showing the difference of accessibility for Trp31.

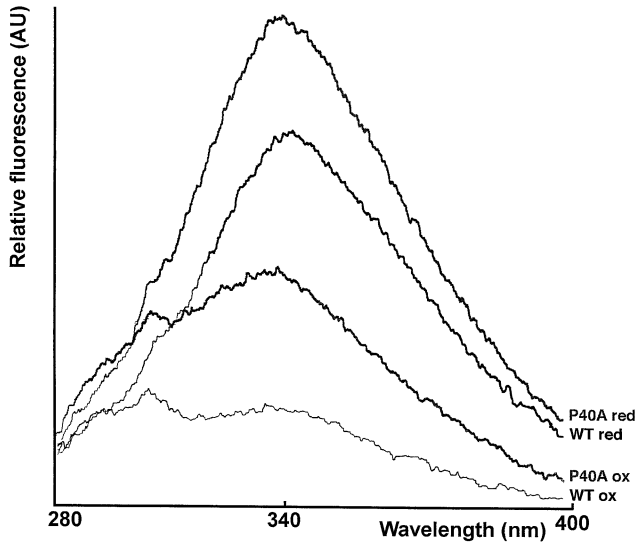

Fig. 5. Fluorescence emission spectra of WT and P40A thioredoxins, in oxidized and reduced forms, at pH 7.2. The samples were excited at 280 nm and the emission was recorded from 290 to 400 nm. Reduction was performed with 5 mM DTT for 10 min.

after reduction, as already reported. On the other hand, the fluorescence emission of both oxidized and reduced P40A was significantly higher than the fluorescence of WT protein, revealing that the conformation is less quenched in the mutant protein.

Both overproduced thioredoxins were submitted to irreversible inactivation assay by heat at 95°C, since *E.coli* WT thioredoxin is known to be remarkably heat stable ($t_{1/2}$ for the oxidized form is ~85°C; Ladbury *et al.*, 1993). Aliquots were taken at different times up to 2 h and tested for their ability

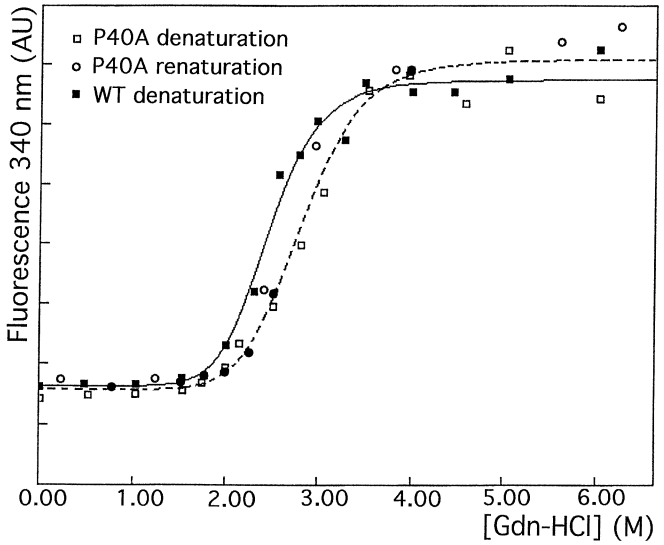

Fig. 6. Guanidine hydrochloride-induced unfolding of WT thioredoxin (solid line) and P40A thioredoxin (dashed line) followed by the change in fluorescence intensity, at 340 nm. Denaturation and renaturation were performed at 25°C in phosphate buffer, pH 7.2.

Table I. Guanidine hydrochloride denaturation parameters for WT and P40A thioredoxins

	$(Gdn–HCl)_m$ (M)	$\Delta G°$ (kcal/mol)	*m* (kcal/mol.M)
WT	2.4	8.9	3.7
P40A	2.8	6.0	2.2

$\Delta G°$ is the free energy in the absence of denaturant, $(Gdn–HCl)_m$ is the denaturant concentration at the midpoint of the unfolding transition and *m* is the dependence of ΔG on denaturant concentration. All the values are derived from data presented in Figure 6.

to activate the NADP–MDH in the presence of DTT. No difference was observed as both proteins exhibited remarkable thermostability, activating the target enzyme with a constant efficiency.

The unfolding of oxidized P40A and WT thioredoxins induced by Gdn–HCl was followed by the change in tryptophan fluorescence emission and CD ellipticity. Addition of Gdn–HCl resulted in a cooperative and reversible unfolding of both thioredoxins (Figure 6). Similar results were obtained when denaturation was monitored by CD at 220 nm (data not shown). The midpoint of the transition curves observed for P40A increased significantly compared with the WT protein (Table I). However, this effect was associated with a decrease in the cooperativity of the folding transition. Therefore, oxidized P40A appears to be less stable by 2.9 kcal/mol than theWT protein, in spite of the unusual increase in the midpoint value.

Enzymatic characterization of P40A

Several tests were used to determine if the mutation modified the activity of the protein. Thioredoxins were reduced either by chemical (DTT) or protein (NADPH–thioredoxin reductase or ferredoxin–thioredoxin reductase) reductants.

Oxidized WT and P40A were tested as substrates for *E.coli* NADP–thioredoxin reductase. The values of K_m and k_{cat} were almost identical for the two proteins (Table II). Hence the mutation did not significantly alter the ability of the protein to be reduced by its specific reductase.

Since *E.coli* thioredoxin was shown to be as efficient as the

Table II. Kinetic constants of WT and P40A thioredoxins

	NADPH–thioredoxin reductase			NADP–MDH activity	
	K_m (μM)	k_{cat} (s^{-1})	k_{cat}/K_m (s^{-1}/μM)	$S_{0.5}$ (μM)	k_{cat} (s^{-1})
WT	3.2	12.5	3.9	5	270
P40A	1.7	10.5	6.2	4.5	230

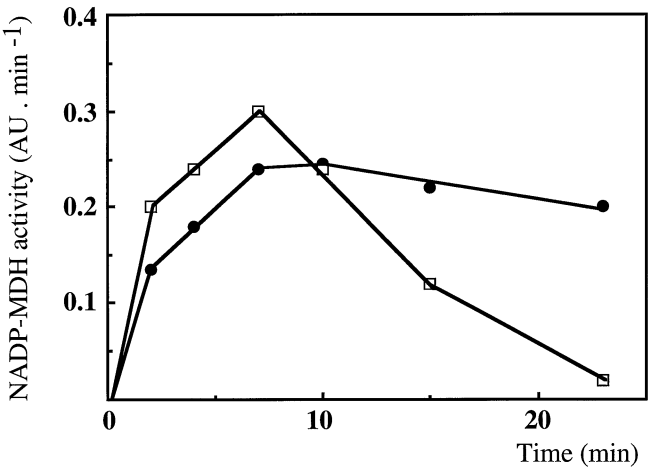

Fig. 7. Thioredoxin-mediated light activation of NADP–MDH at 25°C under air. The activation was performed as described in Materials and methods, at saturating thioredoxin concentration (20 μM). □ WT, ● P40A.

thioredoxin *m* from spinach chloroplasts in the DTT-dependent activation of corn NADP–MDH (Decottignies *et al.*, 1990), the activity of NADP–MDH was monitored at various concentrations of WT and P40A thioredoxins. The concentration required to obtain an activation rate of NADP–MDH equivalent to half of V_{max} ($S_{0.5}$) was identical for the two proteins and the catalytic rates were similar (Table II).

The *in vitro* light activation system mimics the chloroplastic process of activation of assimilatory enzymes under light. It requires the reduction of thioredoxins by the ferredoxin–thioredoxin reductase prior to their action on the target enzymes. When NADP–MDH was activated in this way, identical concentrations of WT and P40A thioredoxins were required to reach the maximum activity (data not shown). However, the behavior of the system at non-saturating concentrations of thioredoxin was different under air and under argon. Under air, the activity of NADP–MDH decreased dramatically after 10 min in the presence of WT protein (Figure 7). This decrease was not observed when the experiment was performed under argon. When P40A was tested in this system, the activity of MDH was stable for at least 20 min under air (Figure 7) and no difference was observed under argon (data not shown).

Discussion

Most thioredoxins have a proline in position 40, which induces a kink in the α2 helix bearing the active site. We have studied the effects of this structural constraint by mutating this residue into an alanine in *E.coli* thioredoxin. The relaxation brought about by this substitution was monitored by a wide array of modeling, biological and biophysical tests. Whereas modeling predicted some structural changes, enzymatic tests revealed only one subtle modification. The biophysical analyses, however, confirmed the effect observed in the simulation.

The overall structure of thioredoxin is conserved in P40A, as predicted by modeling and experimentally confirmed by CD data. The modeling predicts that the kink in α2 helix is suppressed in P40A and that the helix adopts a more regular structure. The active site undergoes a 6 Å shift without any modification of its intimate geometry. This displacement exposes W31 of the active site to the solvent and opens up a cleft located between helices α2 and α3. Such a change induces the deletion of various hydrogen bonds engaged with W31 and W28. In addition, the calculation of the SFE indicates that the mutant is more hydrophobic as W31 becomes more accessible.

These predictions are in total agreement with the experimental data. W31 has been described (Katti *et al.*, 1990) as being located at the surface of *E.coli* thioredoxin, packed against C32 and I75 side chains. NMR relaxation experiments showed that its side chain is more mobile than the W28 side chain (Stone *et al.*, 1993). The role of W31, a strictly conserved residue, has been extensively studied (Holmgren, 1972; Krause and Holmgren, 1991). The fluorescence of the oxidized thioredoxin is strongly quenched by the disulfide and it has been reported that the low fluorescence observed in this form is mainly due to W31 (Slaby *et al.*, 1996). After reduction, a large increase in fluorescence is observed due to a change in fluorescence quantum yield of W28. Modeling data indicate that, in P40A, W31 is less packed in the stucture and the angle between the two tryptophans is modified, so as to bring the two indole rings orthogonal. Hence it could be expected that W31 is less quenched in the oxidized form of the mutated protein and also less efficient in quenching W28 upon reduction, the energy transfer from W28 to W31 being lowered. The fluorescence of both oxidized and reduced forms of P40A is therefore expected to be higher than that in WT, which was observed experimentally. In the same way, it has been reported that the fluorescence of reduced thioredoxin mutants lacking W31 is higher than that of WT, the quenching of W28 by W31 being suppressed (Krause and Holmgren, 1991).

WT thioredoxin is more stable than P40A upon denaturation by Gdn–HCl. However, the effect of the mutation on the transition curve is highly unusual. In almost all known examples, destabilizing mutations are observed to decrease either the transition midpoint or, less frequently, the cooperativity of the unfolding transition. The remarkable feature of P40A thioredoxin is that the transition midpoint increased, indicating that some local structures are actually stabilized by the mutation. However, the overall structure is globally destabilized as reflected by the decrease in the *m* and ΔG values. This might result from several changes, but the main contribution to the destabilization could be the exposure of W31 to the solvent and the unmasking of its natural pocket. The magnitude of this effect (2.9 kcal/mol) is similar to that observed in several thioredoxins with single mutations (Leu78 or Leu42) in the hydrophobic core (Hellinga *et al.*, 1992).

However, according to the modeling data, the residues which are considered to be in interaction with target proteins (residues 33–34, 75–76 and 91–93; Eklund *et al.*, 1984) are not modified in P40A and their hydrogen bonds are not affected by the mutation. This can explain why the biological activities of the mutant are identical with those of WT thioredoxin: neither the ability of the protein to reduce a chloroplastic enzyme nor its reactivity with the bacterial reductase decreased, indicating that Pro40 is not required for maintaining an efficient electron transfer. The main structural effect of the mutation predicted

by modeling, i.e. the movement of W31, is also without consequence on the redox function of the thioredoxin. Krause and Holmgren (1991) had already concluded that W31 is not involved in electron transfer in thioredoxin-dependent disulfide reductions, since its replacement by various amino acids does not dramatically modify the kinetic parameters for the thioredoxin reductase reaction.

The only observed functional difference between the two proteins is the higher stability of the mutant in light activation of NADP–MDH under air. In this system, there is an equilibrium between reduction by illuminated photosynthetic membranes and re-oxidation by air. The decrease in activity observed for WT is usually attributed to the fact that oxidation takes over reduction after 10 min (Decottignies *et al.*, 1990) because the efficiency of the electron transfer is decreasing and oxygen concentration in the medium is increasing. However, it is not known with certainty how activated NADP–MDH is deactivated under oxygen. The enzyme could react with oxygen directly or, alternatively, thioredoxin could be oxidized first and in turn could oxidize NADP–MDH. Our results, which show a different behavior of WT and the mutant protein, suggest the latter chain of events. This interpretation was confirmed by the following experiment. NADP–MDH was activated in the presence of WT thioredoxin and DTT, then the sample was loaded on a gel filtration column in order to separate the enzyme from TRX and DTT as already described (Le Maréchal *et al.*, 1989). NADP–MDH activity was measured after elution and compared with the initial activity of the activated sample. The enzyme was still almost fully active after separation from TRX (data not shown), indicating that it is not directly re-oxidized by air in the course of the separation experiment (~20–30 min, whereas deactivation in the dark takes <2 min). As P40A exhibits a very stable level of NADP–MDH activation, we can therefore conclude that it is less rapidly re-oxidized than WT, a feature which could be of interest in biotechnology.

The behavior of the mutant P40A is convergent with previously reported results. Most of the conserved residues around the active site cysteines have been studied by site-directed mutagenesis in *E.coli* thioredoxin. Among them, the results obtained for the mutant K36E are relevant to our data. Lys36 was first proposed to stabilize the thiolate anion of Cys32 and further reported to be involved in protein interactions. The analysis of the crystal structure of the mutant K36E (Nikkola *et al.*, 1993) showed that the side chain of W31 adopts a new conformation and that the hydrogen bond between the indole ring and the carboxyl oxygen of D61 is suppressed, as observed in P40A. The mutant K36E is less stable than WT, although to a lesser extent than P40A (0.36 kcal/mol). However, this mutant is still a good substrate for thioredoxin reductase and its ability to serve as a reducing agent in the ribonucleotide reductase reaction is not impaired (Gleason *et al.*, 1990; Navarro *et al.*, 1991).

Two other conserved prolines are present in thioredoxin, Pro34 located in the 14-membered ring of the active site and Pro76 which presents the unusual *cis* configuration (Langsetmo *et al.*, 1989). The substitution of P34 for a serine has little effect on either redox activity or thermodynamic stability (Kelley and Richards, 1987; Gleason, 1992), although this residue is strictly conserved in all the sequences. P76 is part of the hydrophobic area close to the S–S bridge and involved in the interaction with target proteins (Eklund *et al.*, 1984). Its mutation into an alanine destabilizes the protein, the Gdn–HCl midpoint for unfolding being lowered (Kelley and Richards, 1987), in contrast to P40A. P76A is reduced by thioredoxin reductase, although with a fivefold-higher K_m and its ability to act as a reducing agent is greatly decreased (Gleason, 1992).

It has already been shown that structurally mutant thioredoxins exhibit perturbed thermodynamic properties (Hellinga *et al.*, 1992) and changes in heat capacity (Ladbury *et al.*, 1995) whereas their biological activity is not affected. Those mutations, located in the hydrophobic core of the protein, were assayed for *in vivo* assembly of filamentous bacteriophage for which the redox activity is not required. The authors concluded that, in thioredoxins, the link between stability and function is not as strong as found in other systems. More recently, the replacement of Trp28 in *E.coli* was reported to induce effects only on thermodynamic stability and not on functional properties (Slaby *et al.*, 1996). P40A is another example of the flexibility of thioredoxin to accommodate amino acid substitution.

Acknowledgments

The authors thank Alain Van Dorsselaer for help with mass spectrometry, Markku Saarinen and Thérèse Malliavin for helpful discussions and Jean-Pierre Jacquot for reading of the manuscript.

References

Brugidou,C., Marty,I., Chartier,Y. and Meyer,Y. (1993) *Mol. Gen. Genet.*, **238**, 285–293.
Buchanan,B.B. (1991) *Arch. Biochem. Biophys.*, **288**, 1–9.
Buchanan,B.B., Schürmann,P. and Jacquot,J.-P. (1994) *Semin. Cell Biol.*, **5**, 285–293.
Chang,T.C., Wu,C.S.C. and Yang,J.T. (1978) *Anal. Biochem.*, **91**, 13–31.
Decottignies,P., Schmitter,J.-M., Miginiac-Maslow,M., Le Maréchal,P., Jacquot,J.-P. and Gadal,P. (1988) *J. Biol. Chem.*, **263**, 11780–11785.
Decottignies,P., Schmitter,J.-M., Jacquot,J.-P., Dutka,S., Picaud,A. and Gadal,P. (1990) *Arch. Biochem. Biophys.*, **280**, 112–121.
de Lamotte-Guéry,F., Miginiac-Maslow,M., Decottignies,P., Stein,M., Minard,P. and Jacquot,J.-P. (1991) *Eur. J. Biochem.*, **196**, 287–294.
Dyson,H.J., Holmgren,A. and Wright,P.E. (1989) *Biochemistry*, **28**, 7074–7087.
Eisenberg,D. and McLachan,A.D. (1986) *Nature*, **319**, 199–203.
Eklund,H., Cambillau,C., Sjöberg,B.-M., Holmgren,A., Jörnvall,H., Höög,J.-O. and Bränden,C.-I. (1984) *EMBO J.*, **3**, 1443–1449.
Eklund,H., Gleason,F.K. and Holmgren,A. (1991) *Proteins*, **11**, 13–28.
Gleason,F.K. (1992) *Protein Sci.*, **1**, 609–616.
Gleason,F.K., Lim,C.-J., Gerami-Nejad,M. and Fuchs,J.A. (1990) *Biochemistry*, **29**, 3701–3709.
Gonzalez Porque,P., Baldensten,A. and Reichard,P. (1970) *J. Biol. Chem.*, **245**, 2371–2374.
Hellinga,H.W., Wynn,R. and Richards,F.M. (1992) *Biochemistry*, **31**, 11203–11209.
Holmgren,A. (1972) *J. Biol. Chem.*, **247**, 1992–1998.
Holmgren,A. (1979) *J. Biol. Chem.*, **254**, 9627–9632.
Holmgren,A., Söderberg,B.-O., Eklund,H. and Bränden,C.-I. (1975) *Proc. Natl Acad. Sci. USA*, **72**, 2305–2309.
Jacquot,J.-P. and Decottignies,P. (1986) *FEBS Lett.*, **209**, 87–91.
Katti,S.K., Lemaster,D.M. and Eklund,H. (1990) *J. Mol. Biol.*, **212** 167–184.
Kelley,R.F. and Richards,F.M. (1987) *Biochemistry*, **26**, 6765–6774.
Krause,G. and Holmgren,A. (1991) *J. Biol. Chem.*, **266**, 4056–4066.
Kunkel,T.A. (1985) *Proc. Natl Acad. Sci. USA*, **82**, 488–492.
Ladbury,J.E., Wynn,R., Hellinga,H.W. and Sturtevant,J.M. (1993) *Biochemistry*, **32**, 7526–7530.
Ladbury,J.E., Wynn,R., Thomson,J.A. and Sturtevant,J.M. (1995) *Biochemistry*, **42**, 2148–2152.
Langsetmo,K., Fuchs,J.A. and Woodward,C., (1989) *Biochemistry*, **28**, 3211–3220.
Langsetmo,K., Fuchs,J.A., Woodward,C. and Sharp,K.A. (1991) *Biochemistry*, **30**, 7609–7614.
Laurent,T.C., Moore,E.C. and Reichard,P. (1964) *J. Biol. Chem.*, **239**, 3436–3441.
Le Maréchal,P., Decottignies,P., Jacquot,J.-P. and Miginiac-Maslow,M. (1989) *J. Chromatogr.*, **477**, 305–314.

Navarro,J.A., Gleason,F.K., Cusanovich,M.A., Fuchs,J.A., Meyer,T.E. and Tollin,G. (1991) *Biochemistry*, **30**, 2192–2195.
Nikkola,M., Gleason,F.K., Fuchs,J.A. and Eklund,H. (1993) *Biochemistry*, **32**, 5093–5098.
Reynolds,A.E., Chesnick,J.M., Woolford,J. and Cattolico,R.A. (1994) *Plant Mol. Biol.*, **25**, 13–21**.**
Russel,M. and Model,P. (1985) *Proc. Natl Acad. Sci. USA*, **82**, 29–33.
Russel,M. and Model,P. (1986) *J. Biol. Chem.*, **261**, 14997–15005.
Schenk,H., Klein,M., Erdbrügger,W., Dröge,W. and Schulze-Osthoff,K. (1994) *Proc. Natl Acad. Sci. USA*, **91**, 1672–1676.
Slaby,I. and Holmgren,A. (1975) *J. Biol. Chem.*, **250**, 1340–1347.
Slaby,I., Cerna,V., Jeng,M.F., Dyson,H.J. and Holmgren,A. (1996) *J. Biol. Chem.*, **271**, 3091–3096.
Stone,M.J., Chandrasekhar,K., Holmgren,A., Wright,P.E. and Dyson,H.J. (1993) *Biochemistry*, **32**, 426–435.
Strehlow,K.G., Robertson,A.D. and Baldwin,R.L. (1991) *Biochemistry*, **30**, 5810–5814.
Tabor,S., Hubert,H.E. and Richardson,C.C. (1987) *J. Biol. Chem*., **262**, 16212
Wetterauer,B., Véron,M., Miginiac-Maslow,M., Decottignies,P.and Jacquot,J.-P. (1992) *Eur. J. Biochem*., **209**, 643–649.

Received May 8, 1997; revised September 9, 1997; accepted September 23, 1997